Report #RU 92-12-B

Superconductors Without Supercomputers: Meeting LARGE Scientific Challenges with small Machines

David J.E. Callaway
Department of Physics
The Rockefeller University
1230 York Avenue
New York, NY 10021-6399
USA

Lectures given at the 17th International Nathiagali Summer College on Physics and Contemporary Needs, Nathiagali, Pakistan, 25 June-9 July, 1992.

Abstract

Nonlinear phenomena can produce unexpected novelties, even in problems which have been studied for many decades. Striking phenomena can be uncovered with very modest computational resources. A simple example of the remarkable effects of nonlinearities is provided by the superconducting intermediate state, whose numerical analysis is discussed here in detail.

Work supported in part by the U.S. Department of Energy under Grant No. DOE-AC01-87ER-40325 Task B.

1. *Prolegomena.*

Future generations of scientists will undoubtedly mark the genesis of numerical simulation as one of the great advances of the twentieth century. After a few days of listening to the lectures at this college, it is hard not to feel a sense of excitement at being a part of this "computer revolution." Yet we should remember that the ultimate goal of this program is *science* and not computation. Computers are a means to an end and are not an end in themselves. One should not be daunted if one does not have access to the largest machines. Indeed, as we will see, new perspectives on classic textbook problems can be obtained with moderate computational resources.

One project which is particular well-suited to small-scale numerical techniques is the study of the magnetic intermediate state in type I superconductors. This formidable problem involves the analysis of highly degenerate ground states and intricate fractal-like patterns on many length scales. Yet for all the complexity of its solution, the problem itself can be formulated with deceptive ease: Consider a large square plate of type I superconductor in an incident perpendicular magnetic field. For sufficiently large field strength, the magnetic field must penetrate the superconductor. The problem is to predict this pattern of penetration.

2. *Background and Synopsis.*

The geometry of the problem considered here is the same as the one used originally [1,2] by Landau in 1937. A square flat plate of superconductor is situated in the xy plane, and a perpendicular field H lies in the $\hat{z}$ direction. The magnetic field approaches a constant at large z.

This early work of Landau predated the Ginzburg-Landau equations [3] by 13 years. It missed the essential difference [4] between type I and type II superconductors and ignores important effects of flux quantization. Still, it survives as a textbook [2] model of the intermediate state in type I superconductors.

Landau predicted [1,2] that the magnetic field must penetrate a square plate of what is now called a "type I superconductor" in a pattern of stripes. In the above geometry, the observed pattern in the xy plane is independent of x and periodic in y (or vice-versa), requiring a complete spontaneous breakdown of the *discrete* $[x \leftrightarrow y]$ symmetry. Subsequent experimental work

[5] revealed that the true situation in type I superconductors is far more baroque, involving patterns on many length scales. The patterns do, however, typically possess a degree of elongation, in *qualitative* agreement with Landau. Indeed, if the magnetic field is applied at an *oblique* angle, the domain patterns align [6] in a fashion resembling his model.

A better theoretical understanding of superconductors follows from the Ginzburg-Landau formalism. The major assumption of the approach [3] is that the free energy density $f(\mathbf{x})$ of a superconductor has an expansion

$$f(\mathbf{x}) = f_n + \frac{1}{2}|\mathrm{D}\psi(\mathbf{x})|^2 + \frac{1}{4}[(|\psi(\mathbf{x})|^2 - 1)^2 - 1] + \frac{1}{2}\kappa^2\mathrm{H}^2(\mathbf{x}) \qquad (1a)$$

where $\psi(\mathbf{x})$ is the order parameter (i.e., the superconductor wave function), $\mathrm{H}(\mathbf{x})$ is the magnetic field, $\mathrm{D} = \partial + i\mathrm{A}$ is the covariant derivative and f_n is the free energy of the normal state. Units are chosen so as to measure

$$\begin{aligned} \mathbf{x} \text{ in units of } \xi &\equiv (\Phi_0/2\pi B_{c2})^{\frac{1}{2}} \\ \mathbf{A} \text{ in units of } &\xi B_{c2} \\ f(\mathbf{x}) \text{ in units of } &B_{c2}^2/2\pi\kappa^2 \\ \mathrm{H}(\mathbf{x}) \text{ in units of } &B_{c2} \end{aligned} \qquad (1b)$$

where ξ is the temperature-dependent coherence length, B_{c2} is the critical field, and $\Phi_0 = 2\pi\hbar c/e^*$ ($e^* = 2e$) is the elementary flux quantum. Minimization of the free energy gives its Euler equations of motion:

$$\mathrm{D}^2\psi + \psi - |\psi|^2\psi = 0 \qquad (1c)$$

$$+ \kappa^2[\partial^2\mathbf{A} - \partial(\partial\cdot\mathbf{A})] = \mathbf{J} \qquad (1d)$$

$$\mathbf{J} = Im[\psi^*\mathrm{D}\psi] \qquad (1e)$$

Note the appearance of the Abrikosov parameter κ. This Ginzburg-Landau formalism is quite general [7] and can be derived [8] from the BCS theory.

3. *Brainpower versus computer power: Simplification before simulation.*

The Ginzburg-Landau equation can be discretized and solved directly, as is shown below in section 4. An elegant simplification occurs through the

use of perturbation theory, and this treatment of the problem is discussed first. This approach was initiated by Abrikosov [4] and was subsequently employed by Lasher [11], Maki, and others [12,10,9]. The basic idea is to expand the vector potential, order parameter, and free energy in a power series in a fictitious parameter ϵ.

$$\begin{aligned} \mathbf{A} &= \mathbf{A}_0 + \epsilon\mathbf{A}_1 + \epsilon^2\mathbf{A}_2 + \cdots \\ \psi(x,y) &= \sqrt{\epsilon}\,(\psi_0 + \epsilon\psi_1 + \epsilon_2\psi_2 + \cdots) \\ \overline{f(x,y) - f_n} &= \overline{f_0} + \epsilon\overline{f_1} + \epsilon^2\overline{f_2} + \cdots \end{aligned} \qquad (2)$$

(Here the bar refers to an xy spatial average). At the final step of the calculation, the parameter ϵ is set to one, and the free energy is minimized over the function space of the order parameter.

More explicitly, the lowest order solution for the order parameter with the necessary symmetry properties can be written as [4]:

$$\psi_0(x,y) = \sum_n^{\infty} C_{n/p}\, exp[-ink_0y - \frac{1}{2}(x - nk_0)^2] \qquad (3a)$$

The parameters $C_{n/p}$ are complex numbers which satisfy the periodicity condition.

$$C_{(n+p)/p} = C_{n/p} \qquad (3b)$$

In addition to these $2p$ independent parameters, the real number k_0 and the integer p itself are arbitrary initially. With the choices implicit in eq. (3), the squared order parameter $|\psi|^2$ is periodic (and ψ itself is quasiperiodic) on a rectangle of $(\Delta x, \Delta y) = (pk_0, 2\pi/k_0)$ coherence lengths. Each such rectangle is penetrated by p units of flux:

$$\Delta x \times \Delta y \times B_{c2} \times \xi^2 = p\Phi_0 \qquad (4)$$

The real parameters p, k_0, and the $2p$ complex parameters $C_{n/p}$ are determined variationally by minimization of the free energy. In the case of a superconducting plate of infinite thickness, the solution [4] is quite simple and can be found analytically:

$$\overline{f(x,y) - f_n} = \frac{1}{2}\kappa^2B^2 - \frac{1}{2}\kappa^2(1 - B)^2/[1 + (2\kappa^2 - 1)\beta] \qquad (5)$$

where B is the xy spatial average of the magnetic flux ($0 < B < 1$) and

$$\begin{aligned} \beta &\equiv \overline{r^4}\,(\overline{r^2})^{-2} \\ B &\equiv \overline{F} \\ F(x,y) &= \overline{F} - \frac{1}{2\kappa^2}[r^2(x,y) - \overline{r^2}] + \cdots \\ r^2(x,y) &= |\psi|^2 \end{aligned} \tag{6}$$

For type II superconductors ($\kappa^2 > \frac{1}{2}$), the perturbative free energy eq. (8) is minimized when β is smallest,

$$\text{Type II}: \beta = \beta_{\min} \approx 1.1596 \tag{7}$$

leading to the prediction of a triangular lattice of flux tubes [4]. In the type I case, ($\kappa^2 < \frac{1}{2}$), the perturbative formula eq. (5) predicts [9-12] a complicated series of patterns with large β, implying large fluctuations:

$$\text{Type I}: \beta \approx 1/(1-2\kappa^2) > 1 \tag{8}$$

Although these type I patterns are generally elongated, they differ in detail from Landau's crude model [10]. The point is that the superconductor flux density r^2 behaves like a quantum "phase space" distribution [9-10]. The x and y coordinates of the plate are essentially Fourier conjugates, like position and momentum in quantum mechanics. The "uncertainty principle" underlying eq. (4) implies that a flux distribution which is independent of one coordinate must be sharply localized in the other, rather than the periodic function envisaged by Landau. Landau's model of type I superconductivity is thus (oddly enough) inconsistent with the Ginzburg-Landau equations.

For the case of a superconducting plate of finite thickness, Eq. (5) becomes [11,9]:

$$\Delta f = \frac{1}{2}\kappa^2 B^2 - \frac{1}{2}\kappa^2(1-B)^2/(\kappa^2 D) \tag{9}$$

where D is a quartic function of the $C_{n/p}$ and also depends upon k_0 and p. For plate thickness d less than a critical scale d_c, the function D is strictly positive and is minimized by a parameter set with p diverging as [9]:

$$p \sim |d - d_c|^{-.5} \tag{10}$$

The patterns generated are displayed in fig. 1. For $d > d_c$, all periods p can occur. This increasing period up to a critical scale d_c is reminiscent of ergodicity and transitions to chaotic behavior in classical mechanics.

It is obviously imperative to go beyond the perturbative formula eq. (9). Yet a numerical simulation must confront a novel phenomenon first reported by Hofstadter [13-16] and elucidated in the next section.

4. *Formulation as a Lattice Gauge Theory: the Hofstadter effect.*

The Hofstadter phenomenon becomes relevant when the Ginzburg-Landau equations are formulated on a lattice. Define complex fields $\psi(m,n)$ and real fields $F(m,n)$ on sites (m,n) of a lattice ($x = ma, y = na$; $m,n = 1,\cdots,L$) with lattice spacing a. When the partial derivatives in eq. (1) are replaced by covariant differences, the resulting lattice equations are

$$\begin{aligned} \psi(m+1,n) + \psi(m-1,n) + U(m,n)\psi(m,n+1) \\ + U^*(m,n-1)\psi(m,n-1) \\ = [\epsilon - a^2|\psi(m,n)|^2]\psi(m,n) \end{aligned} \tag{11}$$

$$\begin{aligned} \kappa^2[F(m+1,n) - F(m,n)] &= J_y(m,n) \\ &= Im[\psi^*(m,n)U(m,n)\psi(m,n+1)] \end{aligned} \tag{12a}$$

$$\begin{aligned} \kappa^2[F(m,n+1) - F(m,n)] &= -J_x(m,n) \\ &= -Im[\psi^*(m,n)\psi(m+1,n)] \end{aligned} \tag{12b}$$

$$U(m,n) = U(m-1,n) \times exp[ia^2 F(m,n)] \tag{12c}$$

where $\epsilon \equiv 4 - a^2$ and the gauge is chosen so that the vector potential lies in the y direction. The lattice spacing a is measured in units of the continuum coherence length. Since the desired solutions fill the xy plane, F and $|\psi|^2$ are taken periodic on a square of size $L \times L$ lattice spacings. Then the

periodicity of the physical currents $J(m,n)$ implies that ψ is in general *quasi-periodic* rather than periodic:

$$\begin{aligned}\psi(m,L) &= \psi(m,1)\\ \psi(L,n) &= \psi(1,n)\\ \times exp[-ia^2 \sum_{m'=1}^{L}\sum_{n'=1}^{n} F(m',n')]\end{aligned} \tag{13}$$

Since $\psi(m+L,n+L)$ is single-valued,

$$a^2 \sum_{m=1}^{L}\sum_{n=1}^{L} F(m,n) = 2\pi p = a^2 L^2 B \tag{14}$$

so B is the flux density per elementary plaquette in units of the *continuum* B_{c2}. Here the integer p gives the number of flux quanta penetrating the $L \times L$ large square.

Equations (11-13), though simple in appearance, imply a plethora of strange phenomena. This complexity can be illustrated by a calculation of the critical magnetic field B_{c2} on a finite lattice. When B exceeds this value, the material goes normal, and the only sensible solution to these equations is the trivial one where $\psi(m,n)$ is vanishes. Near this limit, $\psi(m,n)$ is small, and the nonlinear terms can be neglected. Then

$$\begin{aligned}F_0(m,n) &= constant = B = 2\pi p/a^2L^2\\ U_0(m,n) &= exp[2\pi i \frac{p}{L^2} m]\end{aligned} \tag{15}$$

The equation for $\psi(m,n)$ can be simplified by separating variables, i.e.,

$$\psi_0(m,n) = \sum_{l=1}^{L} g_l(m)\, exp[\frac{-2\pi i l n}{L}] \tag{16}$$

When the nonlinear terms in eq. (11) are dropped, it becomes

$$g_l(m+1) + g_l(m-1) + 2\cos[2\pi(lL - pm)/L^2] g_l(m) = \epsilon\, g_l(m) \tag{17}$$

which is Harper's equation [16]. The boundary conditions eqs. (13 and 14) imply that

$$g_l(m+L) = g_{l-p}(m) \tag{18a}$$

so that

$$g_l(m + L^2/p) = g_l(m) \tag{18b}$$

(it may be necessary to define a "superlattice" [13] if L^2/p is nonintegral). Thus the natural periodicity of the $g_l(m)$ is

$$L^2/p \equiv 1/\alpha \tag{19}$$

where α is the (rational) number of flux quanta per plaquette.

The lattice bulk critical field $B_{c2}(\alpha)$ is determined from the largest eigenvalue $\epsilon_{max}(\alpha)$ of eq. (17) via eq. (14):

$$B_{c2}(\alpha) = 2\pi\alpha/[4 - \epsilon_{max}(\alpha)] \tag{20}$$

Note that $B_{c2}(\alpha)$ is a function of α alone.

The Hofstadter phenomenon [13] occurs when the eigenvalue spectrum of eq. (17) is calculated. The result for $\epsilon(\alpha)$ is a very striking discontinuous "butterfly" pattern, with an intricately organized hierarchical fine structure. From eq. (14),

$$a^2 = (\frac{2\pi}{B})\alpha \tag{21}$$

The continuum limit occurs when the lattice spacing approaches zero at fixed B, implying that the limit of interest is $\alpha \to 0$. But the expected continuum limit

$$\lim_{\alpha \to 0} B_{c2}(\alpha) = 1 \tag{22}$$

is <u>not</u> obtained smoothly, instead occurring along the discontinuous upper boundary of the Hofstadter butterfly. Needless to say, this is unsettling behavior for the continuum limit of a lattice gauge theory, for presumably all thermodynamic functions (and not just B_{c2}) will display rough structure as the continuum is approached.

Two useful properties which follow from eq. (20) are

$$\epsilon_{max}(\alpha) = \epsilon_{max}(1-\alpha) \tag{23a}$$

$$\epsilon_{max}(\alpha + N) = \epsilon_{max}(\alpha) \tag{23b}$$

where N is an arbitrary integer. Then

$$B_{c2}(\alpha) = \frac{\alpha}{1-\alpha} B_{c2}(1-\alpha) \tag{24}$$

From ref. [15] values of $\epsilon_{max}(\alpha)$ can be extracted (see Table 1). A plot of $B_{c2}(\alpha)$ versus α is given in fig. 2. Note that away from $\alpha = 1/2$,

$$\begin{aligned} B_{c2}(\alpha) &\approx 1/(1-\alpha) \\ \epsilon_{max}(\alpha) &\approx 4 - 2\pi\alpha(1-\alpha) \end{aligned} \tag{25}$$

(though neither is ever a continuous function) and $B_{c2}(\alpha)$ increases without bound as α approaches one. When α equals one, eqs. (12) have the trivial solution

$$\begin{aligned} \psi(m,n) &= 1 \\ F(m,n) &= B \end{aligned} \tag{26}$$

[essentially equivalent to having no magnetic field, viz. eq. (24), as $B/B_{c2}(1) = 0$].

5. *Numerical solution of the lattice equations.*

a. Method

The lattice Ginzburg-Landau equations, eqs. (11) and (12), are readily accessible to numerical simulation [23], though it is well to remember the cautionary remarks of section 4. The scheme used here is particularly simple. First, an initial choice of the $U(m,n)$ and $\psi(m,n)$ is made for a given average B. Then eq. (11) is solved by relaxation [i.e., each of the $\psi(m,n)$ is determined from its nearest neighbors]. One hundred sweeps through the lattice prove sufficient. Given the old $U(m,n)$ and $\psi(m,n)$, the new $F(m,n)$ are determined from eq. (12) via a finite Fourier transformation in a single step with B, the average of $F(m,n)$, held fixed. The new $U(m,n)$ are determined, and the process is repeated. Typically about 2,000 loops through the whole algorithm suffice. The usual checks using different starting conditions were made. An easy and adequate initial condition is $F(m,n) = B$; $\psi(m,n) = 1$.

The limit of interest is that of small α, by eq. (21). Yet from eq. (19), the natural periodicity of the system is $1/\alpha$. Thus, $1/\alpha = L^2/p \geq L$. The optimal choice for p is therefore $p = L = 1/\alpha$, and it is used here unless otherwise noted.

b. Vortex arrays in type II superconductors.

One characteristic signature of type II superconductors is the triangular lattice of flux tubes predicted by Abrikosov. The p maxima of $F(m,n)$ per $L \times L$ periodic square are easily seen; their patterns are displayed in fig. 4 for parameter values $B = 0.9$, $\kappa^2 = 10$ and various α. Since a triangular lattice involves irrational tangents, it can never fit exactly on a square lattice; yet the arrays in fig. 3 form fair approximations to a triangular lattice. In fig. 4 the squared distances d^2 between lattice points (taken in units of squared lattice spacing) are plotted versus $1/\alpha$ along with the Abrikosov value $d^2 = \sqrt{4/3}/\alpha$. Reasonable agreement is obtained, though scatter is large. The lattice spacings are equal in the x and y directions, so these triangular "Abrikosov" lattices are a true nonperturbative prediction (compare [18]).

For these same parameter values the xy average $\overline{|\psi|^2} \equiv \rho$ is plotted versus $1/\alpha$ in fig. 5. As the $\alpha \to 0$ continuum limit is approached, the value of ρ scatters discontinuously [as did $B_{c2}(\alpha)$, cf. fig. 2] but clearly approaches a limit. Comparison with continuum values thus requires fairly small α for respectable results. The values for $\beta(\alpha)$ [cf. eq. (7)] are much better: e.g. $\beta(1/24) = 1.1596$.

It is well to note the existence of defect structures in lattice patterns [23]. Recall from eq. (19) that the natural periodicity of a pattern is $1/\alpha$ lattice spacings. If the system size L is not an integral multiple of $1/\alpha$, defect structures due to the period mismatch can occur. Incomplete equilibration can also produce defects. The first problem can be eliminated and the second reduced by using $p = L = 1/\alpha$.

c. B versus H.

The difference between type I and type II superconductors can be highlighted by comparing B, the magnetic flux density inside the superconductor, with H, the applied magnetic field. Here B is an input parameter given by the spatial average of $F(m,n)$, while H in the present units is defined by

$$H = \frac{1}{\kappa^2} \frac{\partial \overline{f}}{\partial B} \tag{27}$$

and can be calculated with an elegant virial theorem [19]. It is important to note that the assumption that $F(m,n)$ is periodic on an $L \times L$ cell implies constraints by eqs. (14),

$$\sum_{m=1}^{L} J_y(m,n) = \sum_{n=1}^{L} J_x(m,n) = 0 \tag{28}$$

For small enough B, eqs. (28) are typically violated, implying that in this limit the only nontrivial solutions to the Ginzburg-Landau equations involve widely-separated magnetic vortices. Thus the plots given in fig. 6 do not continue to $B = 0$.

In fig. (6a), the type II case $\kappa^2 = 10$ is shown. Note that, as expected, H is larger than B and extrapolates to a finite value H_{c1} as B tends to zero. At the boundary point $\kappa^2 = \frac{1}{2}$ between type I and type II superconductors, [fig. (6b)]:

$$\begin{aligned} H(B) &= B, B > B_{c2} \\ &= H_{c2}, B < B_{c2} \end{aligned} \tag{29}$$

while the flux patterns generated are the same as in the type II limit.

The $B(H)$ curve for type I superconductors is more subtle. Figure (6c) displays this function for $\kappa^2 = 0.35$. Note that $B(H)$ is double-valued, with turning points at $H = H_{c2}$ and $H = H_c > H_{c2}$. As is well-known, type I superconductors exhibit "supercooling," leading to a hysteresis loop in the physically realized $B(H)$. Bulk superconductors become normal at $H = H_c$, while the normal state does not become superconducting again until H is lowered to $H = H_{c2} < H_c$. The curve fig. 6(c) is metastable for $B < B_{c2}$,

$$\frac{\partial^2 f}{\partial B^2} = \kappa^2 \frac{\partial H}{\partial B} < 0 \tag{30}$$

Metastability also occurs in the "effective potential" of quantum field theory and in the equation of state of thermodynamic systems (see, e.g., ref. [20]). There, as here, the proper behavior of the system can be determined by a "Landau construction," shown as dotted lines in fig. 6(c).

The size of the metastable region is determined by the ratio H_c/H_{c2}, which is $1/(\sqrt{2}\kappa)$ in the continuum. The metastable region thus becomes more pronounced as κ decreases. The Ginzburg-Landau formalism for type I superconductors [9-12] is probably only valid for H near H_{c2}, and true experimental predictions for equilibrium structures are likely best obtained

ith "simulated annealing" methods such as that applied in [18] to type II perconductors. Flux patterns extracted from the lattice Ginzburg-Landau uations in the metastable region are generally irregular elongated nucleion lumps whose periodicity is that of the $L \times L$ system. Thus the thickness the superconducting plate provides an important scale [9]. Although for asons discussed above Landau's model of flux penetration in type I superductors is incorrect in detail, it may yet have some qualitative validity.

Concluding remarks.

Computers are becoming an integral part of life around the world. They e also indispensable for progress in the sciences. It should be clear from the aterial presented here that advances can be made with computational architecture of modest size. (The calculations described here were performed a Vax Station.) Moreover, much of the work upon which the present forts were based [1] has been extant in the literature over half a century. Even so, it continues to inspire research [21-23]. Possible practical plications of sensitive metastable phenomena in the superconducting intermediate state include [9,10,13], a new type of "dark matter" detector for ementary particle astrophysics. It may also prove useful to view intermediate state superconductors as giant arrays of Josephson junctions with namic boundaries.

cknowledgements

It is a pleasure to thank the International Programs Division of the National Science Foundation for their support. The assistance of K.A. Shoaib, . Saddiq, and M.M. Awais also was invaluable. Discussions with J. Clarke, Deldar, J. Edwards, S. Kharin, M. Khorassani, A. Malek, G.R. Raisali d G. Steinbrecher were very useful in the formulation of these lectures.

Table 1. $\epsilon_{max}(\alpha)$ for selected α.

α	$\epsilon_{max}(\alpha)$
1/2	$2\sqrt{2}$
1/3	$1 + \sqrt{3}$
1/4	$2\sqrt{2}$
1/5	2.96645
1/6	$(5 + \sqrt{21})^{1/2}$
1/8	$[6 + (12 + 8\sqrt{2})^{1/2}]^{1/2}$

1. L.D. Landau, Phys. Z. Sov. 11 (1937) 129 [JETP 7 (1937) 371]; J. Phys. USSR 7 (1943) 99 [JETP13 (1943) 377]; and in Collected papers of L.D. Landau, ed., D. ter Haar (Gordon and Breach, New York, 1967).

2. L.D. Landau and E.M. Lifshitz, Electrodynamics of continuous media (Pergamon, New York, 1984), sec. 57.

3. V.L. Ginzburg and L.D. Landau, Zh. Eksp. Teor. Fiz.20 (1950) 1064.

4. A.A. Abrikosov, Zh. Eksp. Teor. Fiz. 32 (1957) 1442 [JETP 5 (1957) 1174]. [An important numerical error in this paper was corrected by W.H. Kleiner, L.M. Roth, and S.H. Autler, Phys. Rev. 133 (1964) A122]. A.A. Abrikosov, Dokl. Acad. Nauk SSSR 86 (1952) 489.

5. J.D.Livingston and W. De Sorbo, in Superconductivity, Vol. 2, ed., R.D. Parks, (Marcel Dekker, New York, 1969); R.P. Huebener, Magnetic flux structures in superconductors (Springer, New York, 1979); R.N. Goren and M. Tinkham, J. Low. Temp. Phys. 5 (1971) 465; K.P. Selig and R.P. Huebener, J. Low. Temp. Phys. 43 (1981) 37; W. Buck, K.-P. Selig and J. Parisi, J. Low. Temp. Phys. 45 (1981) 21.

6. Yu. V. Sharvin, Zh. Eksp. Teor. Fiz. 33 (1957) 1341 [JETP 6(1958) 1031]; D.E. Farrell, R.P. Huebener, and R.T. Kampwirth, J. Low. Temp. Phys. 19 (1975) 99.

7. S. Weinberg, Prof. Theor. Suppl. 86 (1986) 43.

8. L.P. Gor'kov, Zh. Eksp. Teor. Fiz. 36 (1959) 1918 [JETP 9 (1959) 1364].

9. D.J.E. Callaway, Ann. Phys. (N.Y.) 213 (1992) 166.

10. D.J.E. Callaway, Nucl. Phys. B344 (1990) 627; Nucl. Phys. B (Proc. Suppl.) 17 (1990) 270.

11. G. Lasher, Phys. Rev. 154 (1967) 345; 140 (1965) A523.

12. K. Maki, Ann. Phys. (N.Y.) 34 (1965) 363; J. Pearl, Appl. Phys. Lett. 5 (1964) 65; A.L. Fetter and P.C. Hohenberg, Phys. Rev. 159 (1967) 330; R.P. Huebener, Phys. Rep. C13 (1974) 143; A. Kiendl, J. Low. Temp. Phys. 38 (1980) 277.

13. D.R. Hofstadter, Phys. Rev. B14 (1976) 2239; Godel, Escher, Bach: an eternal golden braid (Vintage, New York, 1989).

14. M. Ya. Azbel, Zh. Eksp. Teor. Fiz. 46 (1964) 929; A.H. MacDonald Phys. Rev. B28 (1983) 6713; R. Rammal and J. Bellisard, J. de Phys. 51 (1990) 2153; A. Moroz, Max Planck preprint MPI-Ph/91-22.

15. Y. Hasegawa, P. Lederer, T.M. Rice, and P.B. Wiegmann, Phys. Rev. Lett. 63 (1989) 907.

16. P.G. Harper, Proc. Roy. Soc. Lond. A68 (1955) 874.

17. D.J.E. Callaway and R. Petronzio, Nucl. Phys. B280 [FS18] (1987), 481; P.H. Damgaard and U.M. Heller, Phys. Rev. Lett. 60 (1988) 1246; D.J.E. Callaway and L.J. Carson, Phys. Rev. D25 (1982) 531; D.J.E. Callaway and A. Rahman, Phys. Rev. Lett. 49 (1982) 613.

18. M.M. Doria, J.E. Gubernatis, and D. Rainer, Phys. Rev. B41 (1990) 6335.

19. M.M. Doria, J.E. Gubernatis, D. Rainer, Phys. Rev. B39 (1989) 9573.

20. D.J.E. Callaway and D.J. Maloof, Phys. Rev. D27 (1983) 406; D.J.E. Callaway, Phys. Rev. D27 (1983) 2974.

21. H. Frahm, S. Ullah, and A.T. Dorsey, Phys. Rev. Lett. 66 (1991) 3067; F. Liu, M. Mondello, and N.D. Goldenfeld, Phys. Rev. Lett. 66 (1991) 3071.

22. P.R. Solomon and R.E. Harris, Phys. Rev. AD3 (1971) 2969.

23. D.J.E. Callaway, Rockefeller preprint, RU-92-5-B.

Figure Captions

Figure 1

Flux patterns for various values of d for $\kappa = 0.5$. Width of picture is 17 coherence lengths.

Figure 2

Critical field $B_{c2}(\alpha)$ versus α (points). The line is the function $1/(1-\alpha)$, displayed for comparison.

Figure 3

Unit cells of vortex lattices for $\kappa^2 = 10$ and $\alpha = 1/8, 1/12, 1/16, 1/20$, and $1/24$; respectively. Lines are drawn to guide the eye.

Figure 4

Squared distance (in units of a^2) d^2 between vortices plotted versus α for regular lattices. Dots show d^2 versus $1/\alpha$ (N.B. $\alpha = 10$ and 13 correspond to square lattices). Abrikosov result $\sqrt{4/3}/\alpha$ shown as straight line.

Figure 5

Average $|\overline{\psi}|^2 = \rho$ versus $1/\alpha$ for $\kappa^2 = 10$ and $B = 0.90$.

Figure 6

B versus H for $\alpha = 1/12$

a) $\kappa^2 = 10$

b) $\kappa^2 = 0.5$

c) $\kappa^2 = 0.35$.

Solid lines denote the calculated curve; dashed lines the "Landau construction."

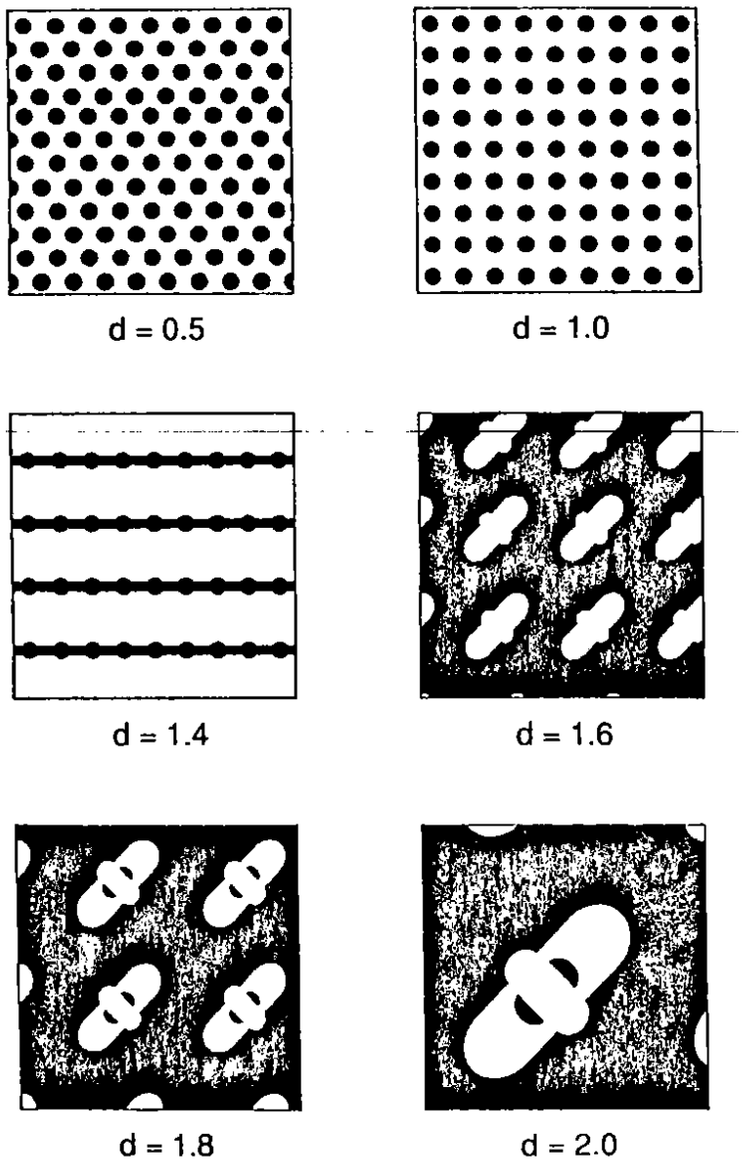

Figure 1.

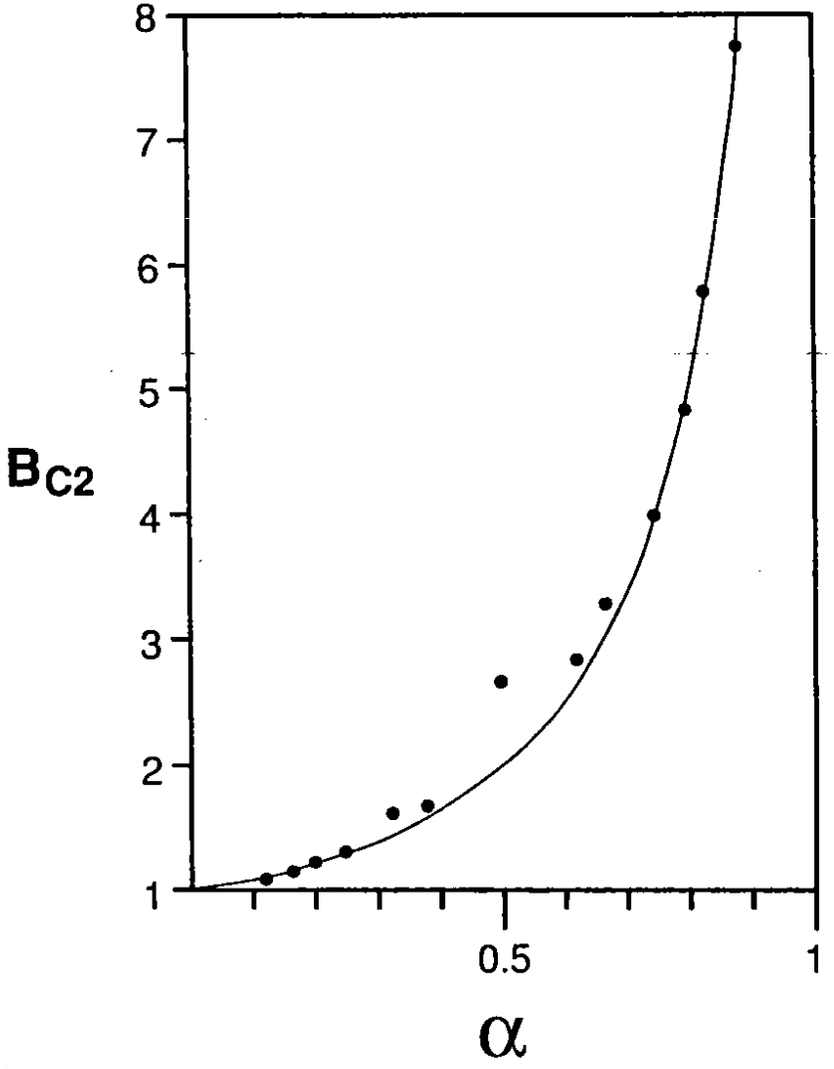

Figure 2.

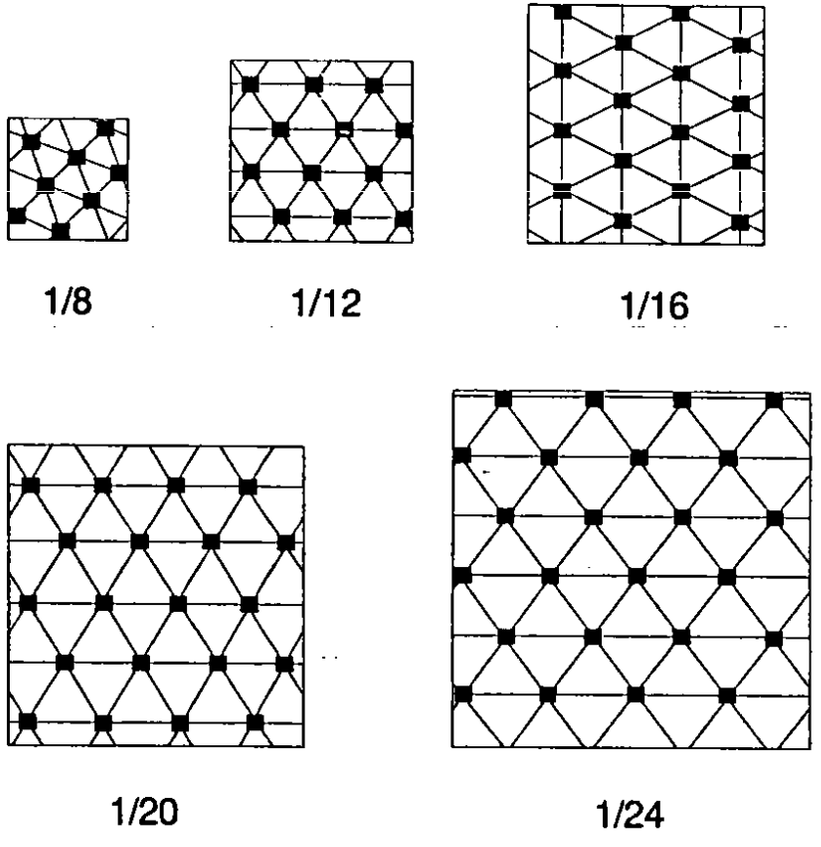

Figure 3.

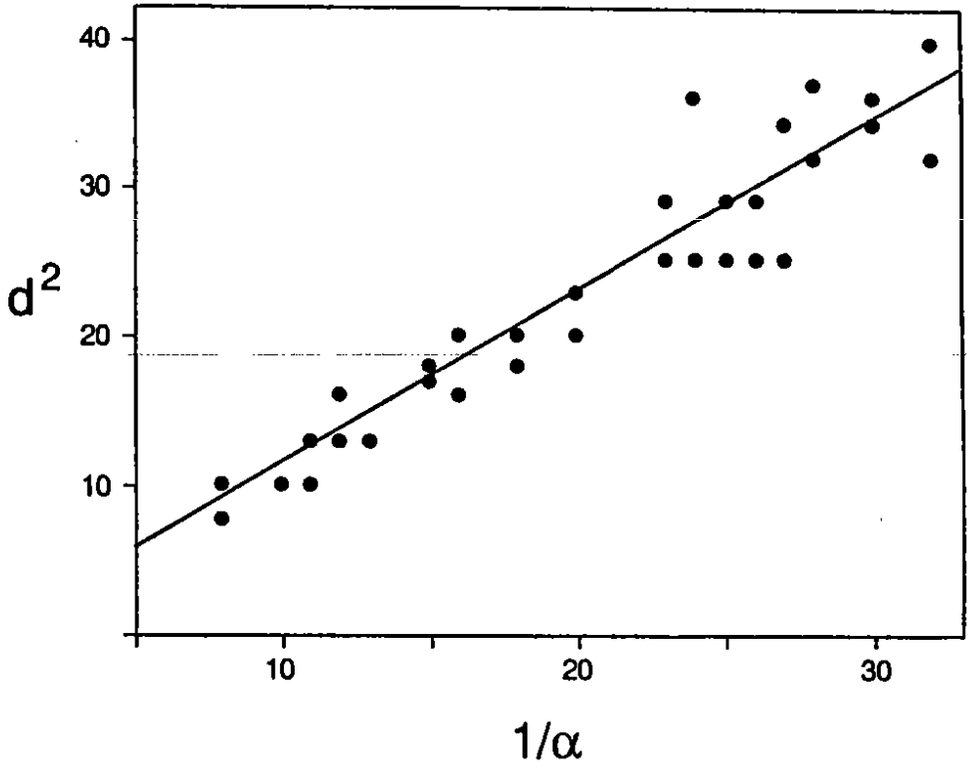

Figure 4.

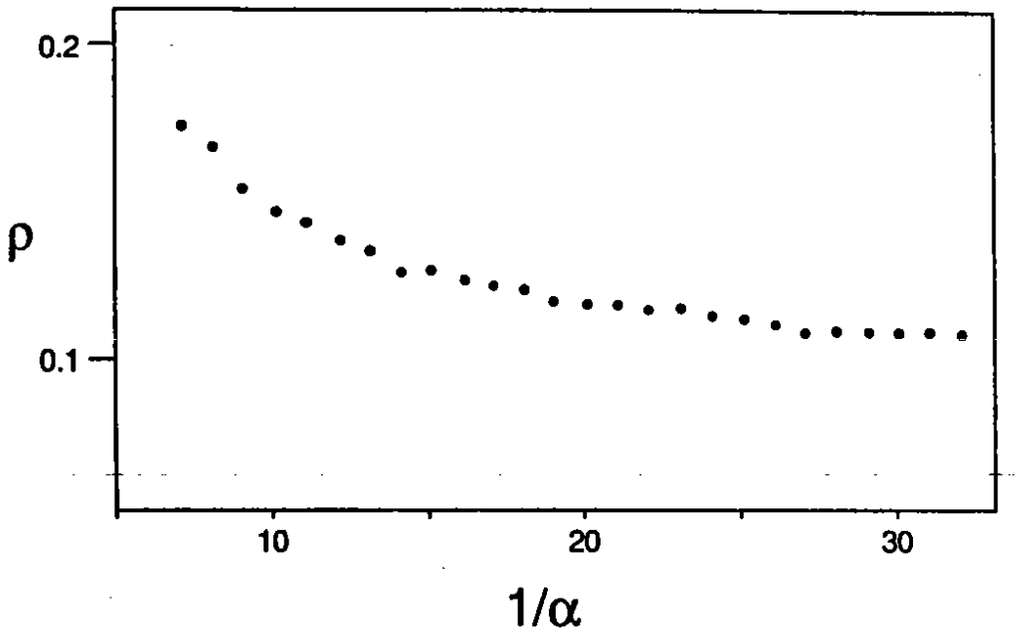

Figure 5.

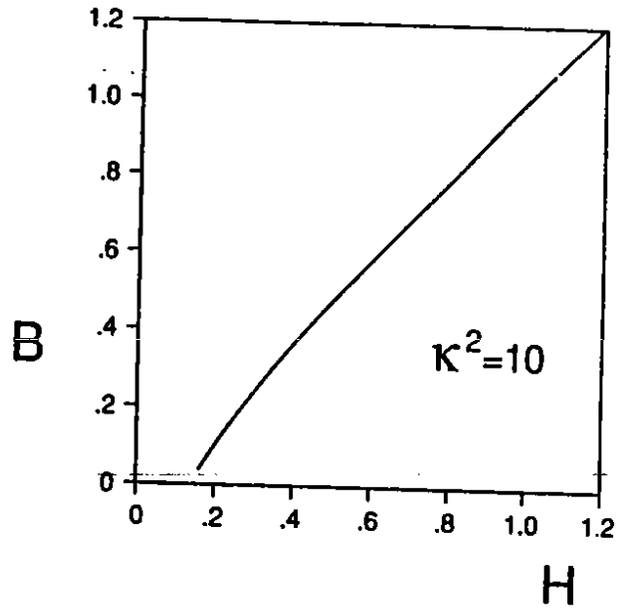

(a)

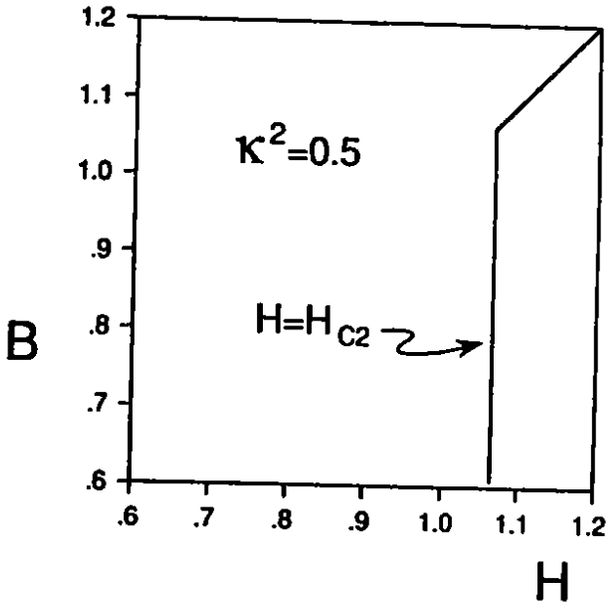

(b)

Figure 6.

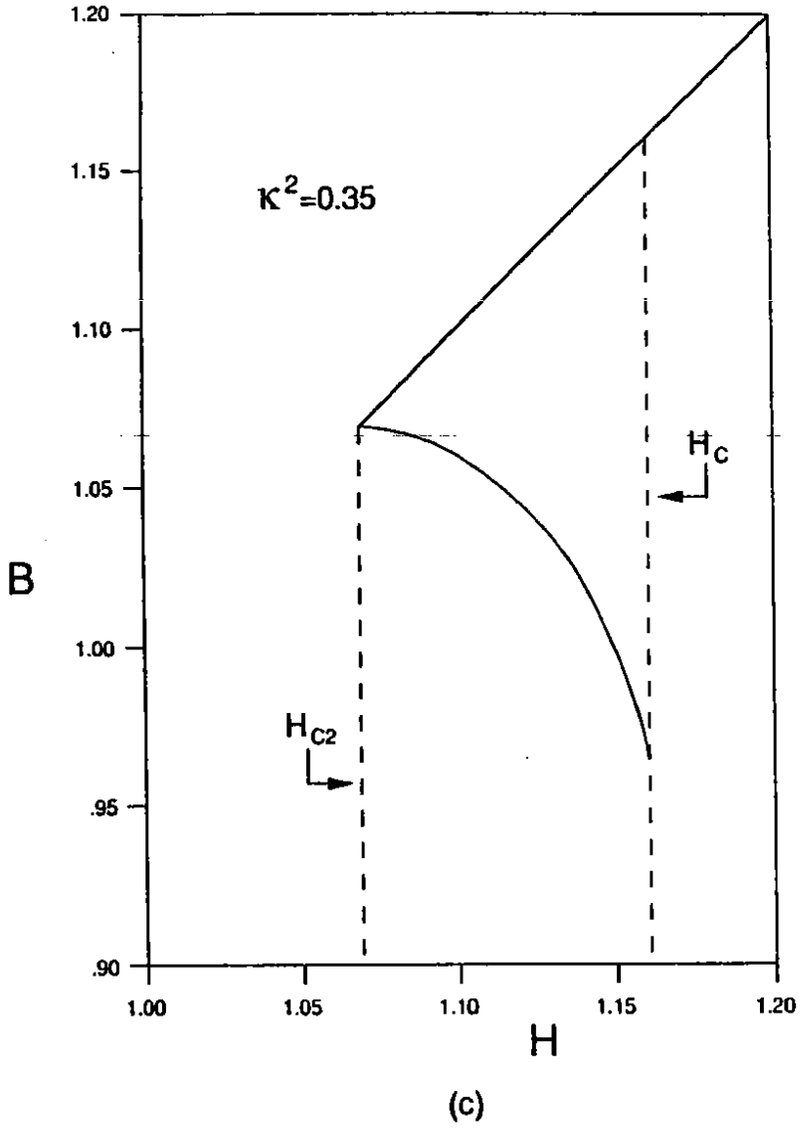
1.20
1.15
1.10
1.05
1.00
.95
.90
B
κ^2=0.35
H_c
H_{c2}
1.00
1.05
1.10
1.15
1.20
H

(c)

Figure 6.